Harmonium: Asymmetric, Bandstitched UWB for Fast, Accurate, and Robust Indoor Localization

Benjamin Kempke, Pat Pannuto, and Prabal Dutta

Electrical Engineering and Computer Science Department
University of Michigan, Ann Arbor, MI 48109
Email: {bpkempke,ppannuto,prabal}@umich.edu

Abstract—We introduce *Harmonium*, a novel ultra-wideband RF localization architecture that achieves decimeter-scale accuracy indoors. Harmonium strikes a balance between tag simplicity and processing complexity to provide fast and accurate indoor location estimates. Harmonium uses only commodity components and consists of a small, inexpensive, lightweight, and FCC-compliant ultra-wideband transmitter or *tag*, fixed infrastructure *anchors* with known locations, and centralized processing that calculates the tag's position. Anchors employ a new frequency-stepped narrowband receiver architecture that rejects narrowband interferers and extracts high-resolution timing information without the cost or complexity of traditional ultra-wideband approaches. In a complex indoor environment, 90% of position estimates obtained with Harmonium exhibit less than 31 cm of error with an average 9 cm of inter-sample noise. In non-line-of-sight conditions (i.e. through-wall), 90% of position error is less than 42 cm. The tag draws 75 mW when actively transmitting, or 3.9 mJ per location fix at the 19 Hz update rate. Tags weigh 3 g and cost $4.50 USD at modest volumes. Harmonium introduces a new design point for indoor localization and enables localization of small, fast objects such as micro quadrotors, devices previously restricted to expensive optical motion capture systems.

I. INTRODUCTION

Indoor localization is a well-researched problem [1], [2]. Prior work spans GSM [3], WiFi [4], [5], Bluetooth [6], [7], ultra-wideband RF [8]–[10], acoustics [11], [12], magnetics [13], LIDAR [14], Visible Light Communication [15], [16], Power Line Communication [17], and more. Systems range from hundreds to hundreds of thousands of dollars, tags and anchors from grams to kilograms, and accuracy from millimeters to meters.

This paper introduces Harmonium, a new RF localization design that provides decimeter-accurate indoor location estimates in real-time with zero warmup period using a tag whose size, weight, cost, and power are inferior only to select RFID-based and tagless systems. Harmonium is the first non-optical system able to both pinpoint and track small, fast-moving objects such as fingers or micro quadrotors and the only system able to do so from a single measurement and in non-line-of-sight conditions. Harmonium employs small RF transmitters (*tags*) that are attached to the device being tracked, fixed receivers (*anchors*) that measure the arrival times of a tag's transmissions, and a multilateration-based TDoA localization engine realized in hardware to solve tag position.

While high-fidelity indoor localization enables a bevy of applications, from precise asset tracking and management to
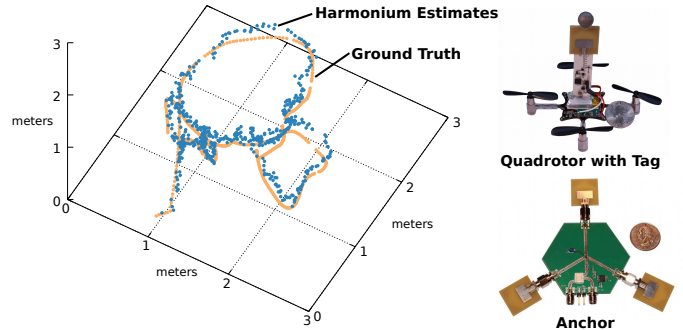

Fig. 1: A Harmonium system reconstructs the flight path of a 19 g quadrotor in a $3\times3\times3$ m space at a 19 Hz update rate using four anchors and a tag that is small (1.5 cm^3), low-cost ($4.50), lightweight (3 g), and low-power (75 mW). Ground truth is acquired using the commercial OptiTrack optical motion capture system. Harmonium tracks the path with 14 cm median error and 46 cm error at the 95th percentile.

novel interaction paradigms, we find the tracking of micro quadrotors, such as in Figure 1, a compelling application as it presents some of the most restrictive requirements for a localization system. Airborne drones require fast, fine-grained localization to navigate indoor spaces. However, they also have very stringent size, weight, and power (SWaP) constraints, limiting payload options. Moreover, small, agile quadrotors draw roughly 200 mW *per gram* simply to remain aloft [18].

Recent work has shown that minimal RFID tags [19], [20] or even systems with no tags at all [21] can achieve decimeter-scale accuracy indoors, meeting the SWaP demands of micro quadrotors. Unfortunately, micro quadrotors impose additional demands beyond SWaP. For one, they are fast. Harmonium is able to track a micro quadrotor traveling at 1.4 m/s, while RFID-based systems have a best-case upper bound of 0.5 m/s [19]. Secondly, they are small, with a total surface area less than 250 cm^2. Tagless systems rely on detecting reflections of the object they are tracking. As objects get smaller and faster, distinguishing them from noise becomes intractable for current systems. Finally, there is a bootstrapping problem. Both RFID and tagless systems optimize for tracking *changes* in position. As a consequence, they either precisely track devices with a constant translation from their actual position or require several seconds of motion to retroactively learn the original position. In contrast, Harmonium position estimates are stateless and achieve full accuracy from the first measurement.
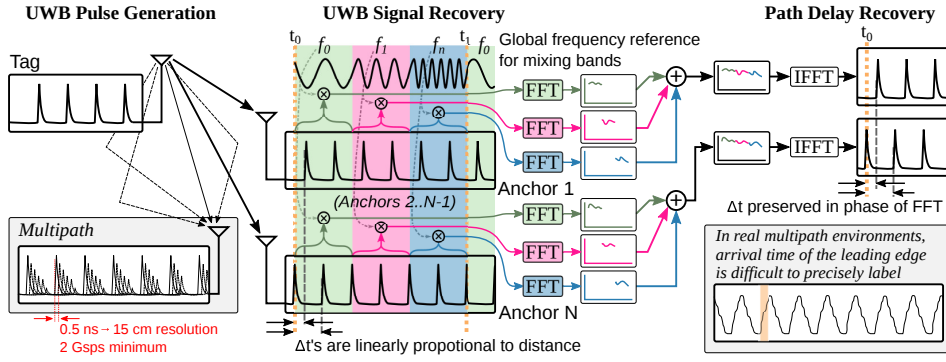
UWB Pulse Generation   **UWB Signal Recovery**   **Path Delay Recovery**

1) **Pulse Generation.** The tag UWB pulse generation design is covered in Section III-B and our exact circuit and implementation are in Section IV-A.
2) **UWB Signal Recovery.** Harmonium anchors employ a novel UWB bandstitching variant, presented in Section III-C, to recover the transmitted signal.
3) **Path Delay Recovery.** Post-processing exploits the frequency diversity enabled by the UWB signal to extract time-of-arrival offset of the pulse train at each anchor node as presented in Section III-E.

Fig. 2: *Harmonium Overview. A mobile tag in free space broadcasts a UWB signal that is captured by anchor nodes. To localize the tag, at least four anchors must capture the tag's signal and determine the relative delay from the tag to each anchor. In complex indoor environments, reflections due to multipath make precisely identifying the arrival time difficult. To achieve 15 cm resolution, direct time-domain UWB recovery would have to sample at 2 Gsps or faster. In contrast, Harmonium adapts bandstitching to recover UWB signals, using frequency-stepped commodity narrowband RF frontends to capture successive chunks of the UWB frequency components. These chunks are combined in the frequency domain to recover the whole signal, and returned to the time domain to find the arrival time at each anchor. This approach encodes the time domain difference in arrival times at different anchors in the phase of the complex coefficients of the Discrete Fourier transform; if a signal is delayed by D samples at one anchor with respect to another anchor, then each complex coefficient of the FFT is multiplied by $e^{\frac{-j2\pi kD}{N}}$, where k is the FFT coefficient index and N is the size.*

Harmonium carves a new niche. It achieves the best SWaP performance of any purely RF-based localization system with self-powered tags at the expense of anchor complexity and system deployability. By maintaining an active ultra-wideband tag, however, Harmonium is able to match or exceed the localization performance of all but costly LIDAR and optical motion capture systems. Harmonium is the only RF-based localization system capable of tracking small, fast-moving objects and is the only localization system capable of tracking them in through-wall conditions.

This paper presents the architecture, design, and implementation of the Harmonium localization system. Our first contribution is an architectural evaluation of various ultra wideband techniques, motivating the Harmonium design decisions. Next, the Harmonium tag introduces a novel UWB signal generation technique, improving the practicality of previous designs by eliminating unneeded components and the performance of previous designs by eliminating noise prior to pulse generation. After that, the Harmonium anchor design presents the first UWB bandstitching architecture, making high-fidelity UWB capture accessible to more traditional RF frontends. The principal contribution of this work, then, is synthesizing these elements to demonstrate Harmonium, the first RF localization system capable of supporting high-fidelity, "through-wall" localization of palm-sized quadrotors indoors.

II. HARMONIUM OVERVIEW

Figure 2 shows an overview of the Harmonium design. A Harmonium system consists of anchors (fixed-location infrastructure) and tags (devices to be localized). Harmonium uses the anchor hardware to observe tag transmissions. Raw data from each anchor is collected at a central location for processing and position estimation. The Harmonium tag produces and transmits a repeating sequence of UWB pulses. The time difference of arrival (TDoA) of these pulses at the anchors is used to estimate the location of a tag.

Anchors estimate the channel's impulse response and determine time-of-arrival by looking for the first observable edge. Distinguishing the line-of-sight path from subsequent reflecting paths requires a high-resolution representation of the channel impulse response. Instead of directly sampling the arriving signal with an extremely high-speed ADC to capture the needed temporal resolution, Harmonium assembles the high-resolution representation by sampling across successive frequency bands. Harmonium adds a frequency-stepped local oscillator to the traditional narrowband radio architecture to collect these snapshots. Once the baseband signal is digitized, a few additional processing steps reconstruct the high-resolution representation from these lower-bandwidth snapshots.

Harmonium processing begins by computing the Fourier transform across all frequency bands to determine the most likely tag pulse repetition frequency. Next, Fourier coefficients are extracted based on the derived pulse repetition frequency. An inverse Fourier transform translates from the frequency-domain Fourier coefficients to the corresponding time-domain representation (the channel impulse response). Harmonium then computes time-difference measurements through analysis of the resulting channel impulse response measurements at each anchor. Finally, the time-difference measurements are used to determine an estimate of the tag's physical location using conventional multilateration techniques.

III. ARCHITECTURAL AND DESIGN CONSIDERATIONS

In time-based localization systems, accurately determining signal arrival time is crucial for accurately estimating position. The time-of-arrival of the line-of-sight path directly depends on the distance between transmitter and receiver. Measuring this time is challenging, however, as the propagation of radio waves in air is extremely fast, 3.0×10^8 m/s. With the speed-of-light propagation of RF signals, even 1 ns of error in estimating a signal's arrival time can result in up to 30 cm of ranging error.

(a) Anchor 1

(b) Anchor 2

(c) Anchor 3

(d) Anchor 4
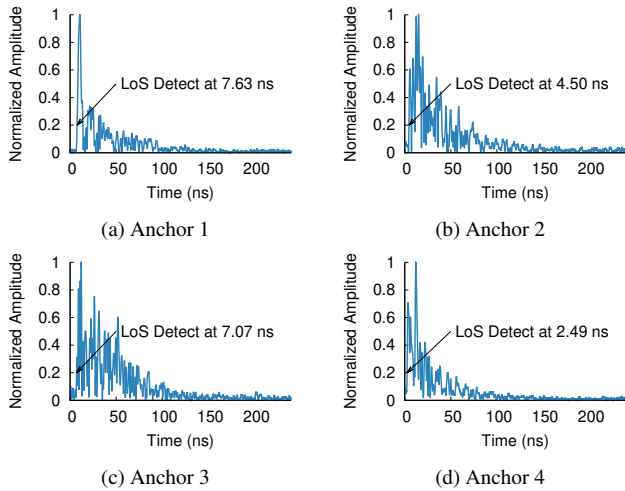
Fig. 3: An example channel impulse response taken by Harmonium. The time-of-arrival for the CIR's leading edge is used as an estimate for the arrival time for the line-of-sight path. Accurately determining the LoS arrival time is the key to determining tag position with low error.

The leading edge of the channel impulse response (CIR) is traditionally used as the measure of true arrival time [22]. However, if the line-of-sight path is too weak or the following peaks arrive quickly after the first, the time-of-arrival estimate can be distorted and difficult to discern. Figure 3 shows a set of RF CIRs observed in a typical indoor environment. These CIRs represent a composite of the magnitudes and arrival times of all propagation paths in the RF channel. This section describes how Harmonium accurately estimates arrival time, the key primitive needed for accurate positioning.

A. Increasing Spatio-Temporal Resolution

The Nyquist-Shannon sampling theorem states that to distinguish features of less than 30 cm requires greater than 1 GHz of sampled bandwidth.[1] The majority of traditional RF frontends are narrowband however, typically offering less than 20 MHz of bandwidth. Such RF frontends do not occupy enough bandwidth to resolve closely-spaced multipath signals. Signals that occupy over 500 MHz of bandwidth are considered ultra-wideband (UWB) and require specially designed RF frontends.

While UWB signals can provide sufficient resolution, there are no available energy-efficient and cost-effective solutions for generating and recovering multi-GHz UWB signals. Most published UWB transmitter designs are impulse-based and are realized in custom chip designs. Similarly, UWB receiver designs for localization applications—those that can capture precise pulse arrival time—either rely on custom VLSI design [23]–[25] or require the use of expensive, fast ADCs [26]–[29]. Additionally, ADCs capable of capturing UWB signals trade off high speed for a low dynamic range, which affects their ability to cancel strong narrowband interferers [30], [31].

---

[1]While there exist "super-resolution" approaches that attempt to model a high-bandwidth impulse response at a finer resolution than allowable by the lower sample bandwidth, they attempt to solve an under-constrained problem with a finite number of multipath components. However, these assumptions do not reflect realistic RF channels in many complex indoor environments.

Harmonium introduces UWB transmitter and receiver designs which do not require costly, high-speed ADCs or custom chip designs. The designs we introduce in this paper allow for the realization of fine-grained spatio-temporal resolution using only commercial off-the-shelf components.

B. Simplified UWB Transmitter Design

UWB transmitter designs either follow a "carrier" or "non-carrier"-based architecture. Carrier-based designs produce UWB transmissions by modulating a high-frequency carrier with a UWB signal, whereas non-carrier UWB directly transmits a high-bandwidth signal without the additional step of carrier mixing. A carrier-based design more closely mirrors common narrowband frontends and more easily accommodates a diverse array of modulation schemes. The carrier generation and mixing circuits, however, are generally more complex and consume $10\times$ or more energy [32], [33] than similar non-carrier designs [34], [35], motivating the use of a non-carrier design.

Non-carrier UWB systems must directly generate extremely high bandwidth signals. The lowest frequency allowed for unlicensed UWB operation indoors in the United States is 3.1 GHz, requiring the design of a signal generator with frequency content in excess of 3.1 GHz. Recent work leverages the step recovery effect of modern RF BJT transistors to create short, ultra-wideband pulses to produce over 4 GHz of bandwidth [36]. These show distinct advantages over previous step recovery diode (SRD) [37] or avalanche transistor designs which either produce insufficient bandwidth [38] or also use expensive SRDs [39].

To be effective, previous designs require a microstrip differentiator for UWB pulse shaping, specifically to limit the UWB pulse's duration. Unfortunately, microstrip differentiator geometries are difficult to design on uncontrolled dielectrics such as FR4 and require complex layout expertise. The Harmonium architecture, however, does not require the use of short pulse durations. Figure 6 shows Harmonium's final tag design, with a number of modifications from Hantshcer's original UWB pulse-generation circuit [36] that enable its low-cost and high-bandwidth pulse generation with low active energy consumption and simplified layout constraints.

C. Recovering UWB and the Time/Frequency Duality

Due to the speed-of-light propagation of UWB signals in air, very stringent requirements are imposed on the receivers used in UWB localization systems. These receivers not only need to measure the time-of-arrival of the line-of-sight path, but they also need to differentiate the effects of the line-of-sight path from those of any following propagation paths. Many different receiver architectures have been proposed and evaluated in prior work for accurately measuring UWB time-of-arrival.

One such receiver architecture leverages the use of multi-Gsps ADCs to estimate UWB time-of-arrival. However, the direct use of an ADC only allows for a minimum time resolution equivalent to that of the ADC's sampling rate. For example, a 1 gigasample per second—1 ns per sample—ADC can only sample the channel impulse response to a resolution of 30 cm.
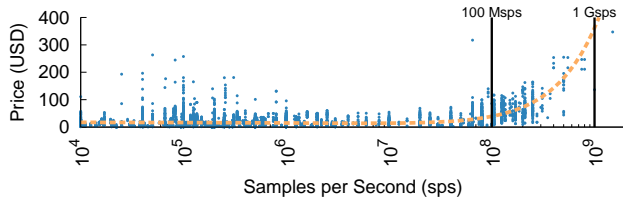
Fig. 4: ADC price versus sampling speed. We scrape all 9,716 of the available ADCs from DigiKey and collect the price per unit for the best bulk rate, discarding products only available in very small quantities (those with no bulk option available). There exists a super-linear relationship between price and sampling rate above about 100 Msps, which is required for traditional UWB anchors. Careful selection of ADC sampling rate is necessary for cost-effective anchor design.

As sampling rate increases beyond 100 Msps, ADC cost grows rapidly. Figure 4 scrapes Digi-Key, sampling 9,716 ADCs, and finds a super-linear relationship between price and sampling rate. In addition, there is a tradeoff between sampling rate and the bit depth of high-speed ADCs. Many multi-Gsps ADCs are restricted to at most 8 bits of resolution, which limits the dynamic range of their measurements and reduces accuracy in the presence of strong narrowband interferers. The following sections consider two approaches to reduce the required ADC sampling rate in UWB time-of-arrival receivers.

1) Segmentation in the Time Domain: Time domain "sub-sampling" achieves similar time-domain resolution to multi-Gsps techniques by sampling different portions of a UWB signal across successive repetitions [36], [40]. This approach uses a special circuit element called a *sampling mixer*. A sampling mixer samples the magnitude of an incoming signal over a short period of time, typically about 1 ns, and triggers at a rate either slightly higher or lower than the UWB signal's repetition frequency to construct a representation of the channel impulse response over the course of many cycles, as Figure 5a shows.

Sub-sampling techniques have been shown to reduce the ADC requirements for UWB signals with low bandwidths. Yet, time segmentation approaches have high dynamic range (ADC bit-depth) requirements in the presence of strong narrowband interferers [41]. Finally, sampling phase detectors are a boutique component only used in specialized radio receiver hardware, making their use in commodity systems costly.

2) Our Approach: Segmentation in the Frequency Domain: The Fourier series provides another route to construct a high-resolution time-domain representation without the use of high-speed ADCs. A signal's equivalent time-domain representation can be reconstructed with just the amplitude and phase for each of the signal's Fourier coefficients. Each Fourier coefficient can be measured independently, either by parallel ADCs [42] or by stitching together successive measurements across different bandwidths from a single ADC [8], [43]. This allows for the use of slower ADCs with higher dynamic range like those more traditionally found in narrowband radio architectures.

Prior frequency segmentation systems (also called *bandstitching*) use narrowband radios comparable in design to current software-defined radios. To change the frequency band of interest, a PLL is programmed to tune the local oscillator to
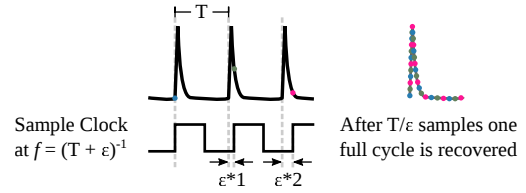
(a) Time Segmentation
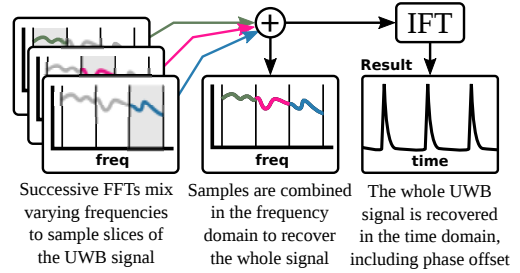
(b) Frequency Segmentation

Fig. 5: Illustration of time and frequency segmentation techniques which can be leveraged to reduce the ADC speed required for UWB time-of-arrival estimation. By sampling at a rate just below the transmitted pulse repetition frequency, a time-stretched representation of the received signal can be reconstructed at a time resolution equivalent to a direct sampling approach. Alternatively, frequency segmentation can be used to construct the equivalent time-domain representation by successively sampling different bandwidths, stitching them together in the frequency domain, and applying the inverse Fourier transform to recover the time domain representation.

a different frequency, changing the center frequency of the narrowband receiver, as shown in Figure 5b. Extending the bandstitching concept to recover UWB signals only imposes additional requirements on the tuning range of the local oscillator. Ultra-wideband VCOs are commercially available, but tend to be costly. Alternatively, wideband frequency synthesizer chips such as the ADF4355 enable low-cost local oscillator generation with the flexibility of a wide tuning range.

Harmonium is the first localization system which extends bandstitching to ultra-wideband bandwidths. Harmonium utilizes a custom-built wideband frequency ramp generator based on the ADF4159 to generate the carrier necessary for band-stitching across such a wide bandwidth. In addition, Harmonium demonstrates the viability of high-speed signal processing required for bandstitching, enabling real-time position estimation using generic PC hardware.

D. Bandstitching for Narrowband Interference Cancellation

The wide bandwidth afforded by UWB systems increases the risk of collision with narrowband systems occupying portions of the same bandwidth. Systems which are unable to segment the reception of UWB signals across frequency must rely on high dynamic range in order to resolve the interfering signals. By segmenting across frequency, Harmonium is able to cancel out narrowband interference by dropping observations which are corrupted by powerful narrowband interference. By leveraging the sparse structure of the channel frequency response, compressive sensing techniques [44] can be used to recover lost observations due to narrowband interference.
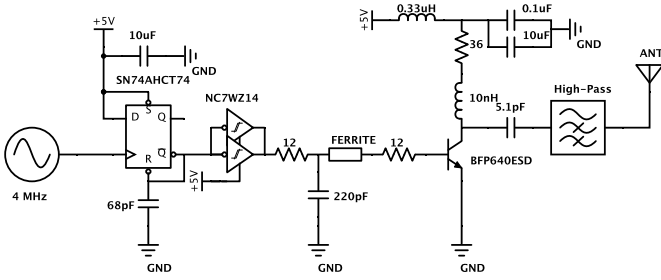
Fig. 6: Tag circuit diagram showing the detailed interconnection between the oscillator, monoflop generator, and BJT transistor. Additional passives are necessary for FCC-compliant pulse shaping. Total tag cost in modest quantity is approximately $4.50 per tag.
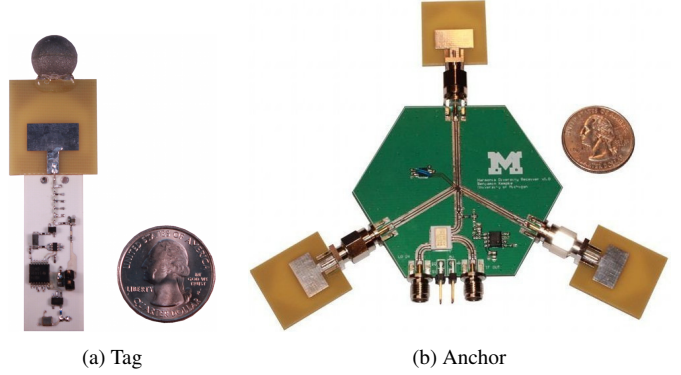

(a) Tag   (b) Anchor

Fig. 7: Harmonium tag and anchors. Tags measure 2.2 cm x 6.3 cm, contain pulse generation circuitry, and are printed on Rogers 4350 PCB substrate. Anchors consist of a centralized local oscillator (LO) frequency generator and separate RF front-ends for down-converting and digitizing the received pulse signals measured at each anchor.

E. Measuring Time with UWB Pulse Trains

Recall that the goal is to precisely capture the time between when a signal is sent from a transmitter and is received by an anchor. There is no synchronization between tags and anchors, which means that tags cannot simply send a single pulse. Rather, tags send a continuous pulse train and anchors compute a phase offset from a shared, global time reference. Since the signal is periodic, this offset will alias if the path delay is longer than the period. In practice, this means that the pulse repetition frequency defines the maximum distance between a tag and anchor that Harmonium can measure. While the interval between pulses can be extended to improve range, this reduces receiver SNR, affecting system performance.

F. From Time to Position

From the base UWB receiver architecture, Harmonium obtains the precise time that pulses are received at each anchor according to the anchor's frame of reference. For this reason, Harmonium anchors all share a tightly synchronized, global time reference. Anchors calculate the offset between the arrival of the tag's transmitted pulse and the global clock pulse.

Calculating position based on time-difference-of-arrival (TDoA) is well-known as multilateration, and uses the same principles used by GPS to perform geolocation. Algorithms have been developed to determine location in three dimensions based on the addition of one or more time-of-arrival estimates [45]–[48]. To minimize the effect of antenna cross-polarization, which can substantially attenuate a signal, Harmonium uses three antennas at each anchor and computes the tag's position using the earliest time-of-arrival at each anchor.

IV. IMPLEMENTATION

One contribution of the Harmonium architecture is that it does not require costly or hard-to-source components and can be realized using only commodity parts. This section presents our implementation of the Harmonium design.

A. Tag Design (Figure 6, Figure 7a)

Harmonium tags produce high-bandwidth pulses using the step recovery effect of common RF bipolar junction transistors (BJTs) [49]. The step recovery effect creates a fast (sub-ns) state-change transition in semiconductor stack-ups due to the quantum

effects of semiconductors recovering from a saturation condition. These fast state-change transitions (low- to hi-voltage or hi- to low-voltage) exhibit bandwidth exceeding 4 GHz, making them well-suited for generating UWB signals.

A crystal oscillator is first used to generate the stable pulse repetition frequency necessary for accurate channel impulse response characterization. This oscillator triggers a monoflop to generate a short-duration (multi-ns) driving signal for the NPN transistor. This short-duration pulse needs to be long and strong enough to drive the transistor into saturation. Once in saturation and the driving signal has transitioned back low, the BJT continues to bleed off charge until the observed step recovery effect takes place. The sharp transition from the conducting to non-conducting states cause a sharp rise in the output voltage present at the transistor collector. Finally, a DC-blocking capacitor and 9th-order Chebyshev low-pass filter are used to attenuate unnecessary low-frequency components to generate FCC-compliant UWB signals. Figure 6 shows a schematic of our tag design.

Figure 7a shows the fabricated pulse generator tag. The tag PCB is constructed using a Rogers 4350 PCB laminate material. The tag is set to generate a pulse train at a 4 MHz repetition frequency using a crystal oscillator. This pulse repetition rate allows for channel delay spreads of up to 250 ns, which we experimentally determine to be adequate for many indoor environments. The fabricated tag occupies 1.5 cm^2, weighs 3 grams, has an active power draw of 75 mW, and costs only $4.50 USD in modest volumes.

B. Anchor Design (Figure 7b)

Each anchor uses three UWB antennas [50] to receive tag transmissions and provide antenna diversity, which has been shown to improve ToA estimation performance in prior work [51]. An RF switch selects different antennas over successive localization measurements. The switched antenna then feeds an LNA and mixer circuit to enable bandstitching at each anchor. Each anchor mixer is fed from a central frequency-stepped local oscillator source to facilitate synchronous bandstitching across

all four anchors. The local oscillator (LO) signal generation board uses an ADF4159 frequency synthesizer that controls the frequency of an RFVC1802 wideband VCO. The LO sweeps from 5.312 GHz to 4.32 GHz in 32 MHz steps. With an intermediate frequency of 990 MHz at each anchor, this in approximately 1 GHz of bandstitched bandwidth from 3.33 GHz to 4.322 GHz.

The resulting mixed intermediate frequency (IF) signal from each anchor returns to a dedicated USRP1 [52] front-end for final down-conversion, digitization, filtering, and data transport to an attached PC. The DBSRX2 daughterboard first converts the 990 MHz IF signal to baseband for ADC sampling. The USRP1 uses 64 Msps baseband ADCs with a bit depth of 12 bits for each of the baseband quadrature channels (in-phase and quadrature-phase). Since the USRP1 uses USB 2.0 to transfer baseband data to the host PC, the resulting 64×10^6 Msps $\times$ 12 bits/sample $\times$ 2 channels = 1536 Mb/sec of baseband data is too much to pass unprocessed to the host PC. Instead, the raw baseband data is comb filtered and decimated to decrease the overall bandwidth required of the host PC data interface.

All signal processing and LO interfacing logic is implemented using a custom FPGA image loaded onto the USRP1's Spartan 3 FPGA. The system repeatedly sweeps the entire bandwidth sequentially across all three antennas, producing localization estimates at 19 Hz. The anchors used in this evaluation cost approximately $750 each due to the high cost of COTS SDRs, yet these could conceptually be replaced with a custom SDR implementation to significantly reduce anchor cost. This, coupled with the advent of inexpensive, integrated wideband synthesizer/mixer RFICs such as the RFMD RFFC5072 could reduce anchor cost to $100.

C. Signal Processing Backend

Signal processing starts in the USRP1's FPGA fabric by performing comb filtering and decimation to achieve a data rate sustainable between the radio and PC. Comb filtering attenuates noise and other sources of interference that occur at frequencies that are not multiples of the pulse repetition frequency. This filtered and decimated data is then post-processed to obtain an estimate of the true pulse repetition frequency with an accuracy of 0.004 Hz. Once the pulse repetition frequency is known, amplitude and phase measurements can be obtained by extracting them from the recorded baseband data. Additional phase and amplitude calibration is performed based on pre-deployment calibration data to avoid errors attributable to manufacturing differences between the anchors.

Once the spectral characteristics have been obtained for each harmonic in the bandwidth of interest, the channel frequency response measured at each anchor can be transformed to the equivalent time-domain representation using the inverse DFT. Time-of-arrival of the line-of-sight path is estimated as the 20% height of the CIR's leading edge [22]. Finally, time-of-arrival estimates from all four anchors are combined to obtain an estimate of the tag's position.

V. EVALUATION

We evaluate the Harmonium prototype on precision, accuracy, consistency, and system burden—weight, volume, and power requirements. We conduct all experiments in an approximately rectangular $4.6 \times 7.2 \times 2.7$ m room in a commercial building with heavy multipath characteristics. We assign the origin to a floor-level corner and coordinate axes run along each of the orthogonal wall edges. We install a NaturalPoint OptiTrack motion capture system [53], calibrated to a sub-mm accuracy, in the room to provide ground truth measurements for all experiments. Harmonium achieves a median 14 cm error with a 90th-percentile error of 31 cm and median precision of 9 cm while drawing only 75 mW with a 3 g tag.

A. Stationary Precision (Figure 8)

We place a tag at fifteen fixed positions in space, taking roughly forty samples at each position, to measure the typical magnitude of position estimation noise from system and environmental noise. Figures 8a and 8b show ground truth locations and point cloud estimates for each position in line-of-sight (LOS) conditions. Harmonium achieves 14 cm median error with 9 cm median precision.

We next consider the through-wall performance by obstructing the LOS path to each anchor with drywall. This experiment evaluates Harmonium's performance when deployed in a visually unobtrusive manner. As Figures 8c and 8d show, Harmonium accuracy falls only slightly, to 16 cm median error and 13 cm median precision, in the through-wall case.
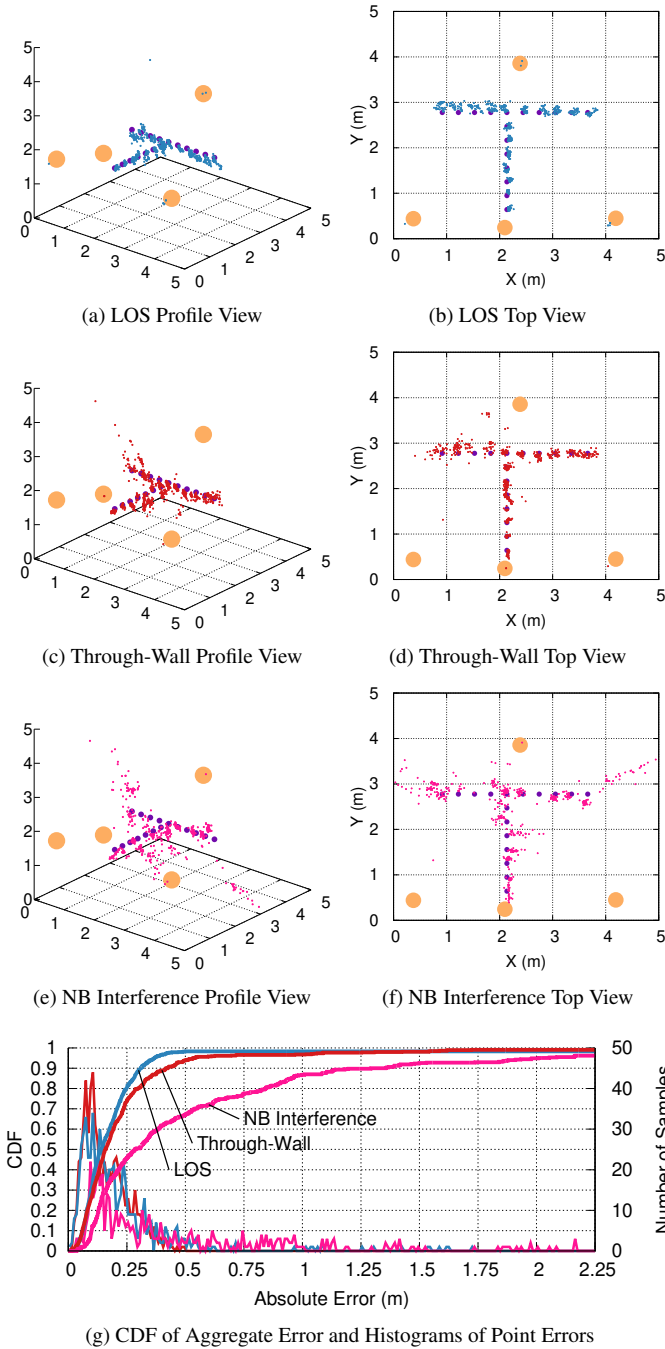
For the final stationary experiment, shown in Figures 8e and 8f, we introduce a strong narrowband interferer by radiating a modulated 3.6 GHz signal with a nearby USRP. While the overall median error and precision, 28 cm and 17 cm respectively, continue to perform well, certain physical spaces fail completely, such as position #14 which exhibits 217 cm median error with 38 cm precision. Recently, the first commercially-accessible UWB transceiver, the DecaWave DW1000 [54] was released. While building and evaluating a complete localization system using DecaWave to compare against is beyond the scope of this paper, we do validate one of our previous claims that motivated the bandstitching-based approach, and find that a pair of DecaWave chips fail to communicate in the presence of the same narrowband interferer.

These experiments give a sense of the consistency of position estimates obtained with Harmonium. Due to the approximately normal distribution of position estimation noise across each dimension, a reduced variance in position estimation noise can be obtained by taking a moving average of position estimates. While this will decrease the average position error, it has a cost of reduced position update rate. All following experiments are performed using raw position estimates without any temporal filtering of the data.

B. Quadrotor Flight Path Reconstruction (Figure 9)

We next evaluate Harmonium in a motivating application domain: real-time tracking of indoor quadrotors. The Crazyflie Nano is a 19 g, $9 \times 9 \times 2$ cm quadrotor with a 170 mAh battery
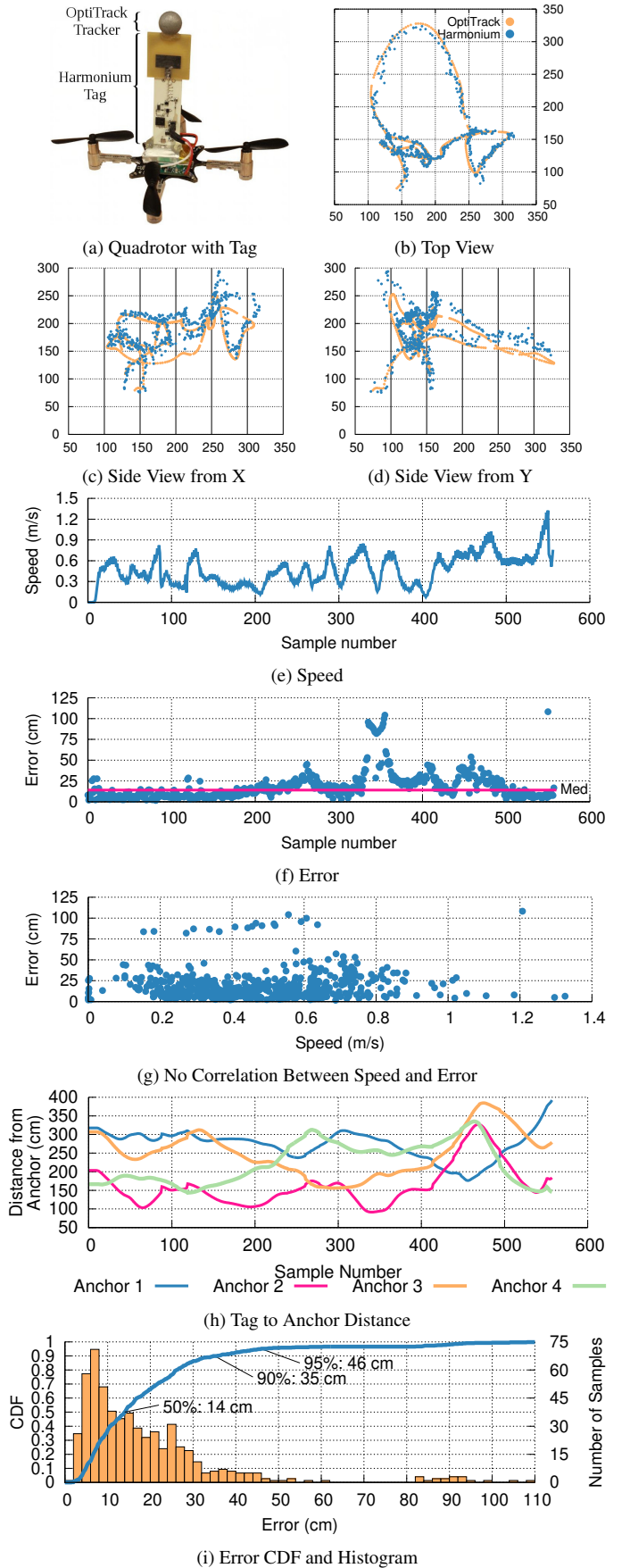
(a) LOS Profile View

(b) LOS Top View

(c) Through-Wall Profile View

(d) Through-Wall Top View

(e) NB Interference Profile View

(f) NB Interference Top View

(g) CDF of Aggregate Error and Histograms of Point Errors

Experiment	Median Precision	90th %ile Precision	95th %ile Precision	Median Accuracy	90th %ile Accuracy	95th %ile Accuracy
LOS	9 cm	16 cm	37 cm	14 cm	31 cm	37 cm
Through-Wall	13 cm	38 cm	51 cm	16 cm	42 cm	53 cm
Interference	17 cm	43 cm	107 cm	28 cm	136 cm	201 cm

(h) Key metrics

Fig. 8: Static position estimates in varying environments. We place Harmonium at fifteen known locations and capture roughly 40 position estimates at each point. First we capture the line-of-sight (LOS) base case. Then we evaluate through-wall performance by occluding the anchors with drywall. Finally, we introduce a narrowband interferer strong enough to completely knock out a commercial UWB system and observe Harmonium's performance. Harmonium exhibits minor (2 cm) performance degradation in the through-wall case and only 2× loss in median accuracy in the face of strong narrowband interference, demonstrating the efficacy of Harmonium's bandstitching architecture.

(a) Quadrotor with Tag

(b) Top View

(c) Side View from X

(d) Side View from Y

(e) Speed

(f) Error

(g) No Correlation Between Speed and Error

(h) Tag to Anchor Distance

(i) Error CDF and Histogram

Fig. 9: Point-cloud of location estimates and CDF of location error tracking a quadrotor. Harmonium shows no increase in error up to the 1.4 m/s top speed of the quadrotor, nor does Harmonium severely burden the quadrotor's ability to fly, adding less than 15% to the mass.

and a payload capacity of only 10 g [55]. The existing motors and electronics draw approximately 1400 mA (5180 mW at 3.7 V) while hovering, so the Harmonium tag power draw only reduces flight time by 1.4%. The additional weight dominates the additional power draw required for the Crazyflie to maintain hover. With an approximate 200 mW/g of additional payload, the quadrotor would require an extra 600 mW of power to maintain hover with an affixed Harmonium tag.

We affix a Harmonium tag and fly the quadrotor around the indoor space. Figure 9 captures a trace of this flight. The flight exhibits a median error of 14 cm and 90th percentile error of 35 cm. Empirically, significant errors are clustered in space and time, suggesting that there is a physical root cause and that temporal filtering will be insufficient to resolve the errors. We explore this observation further in the next experiment.

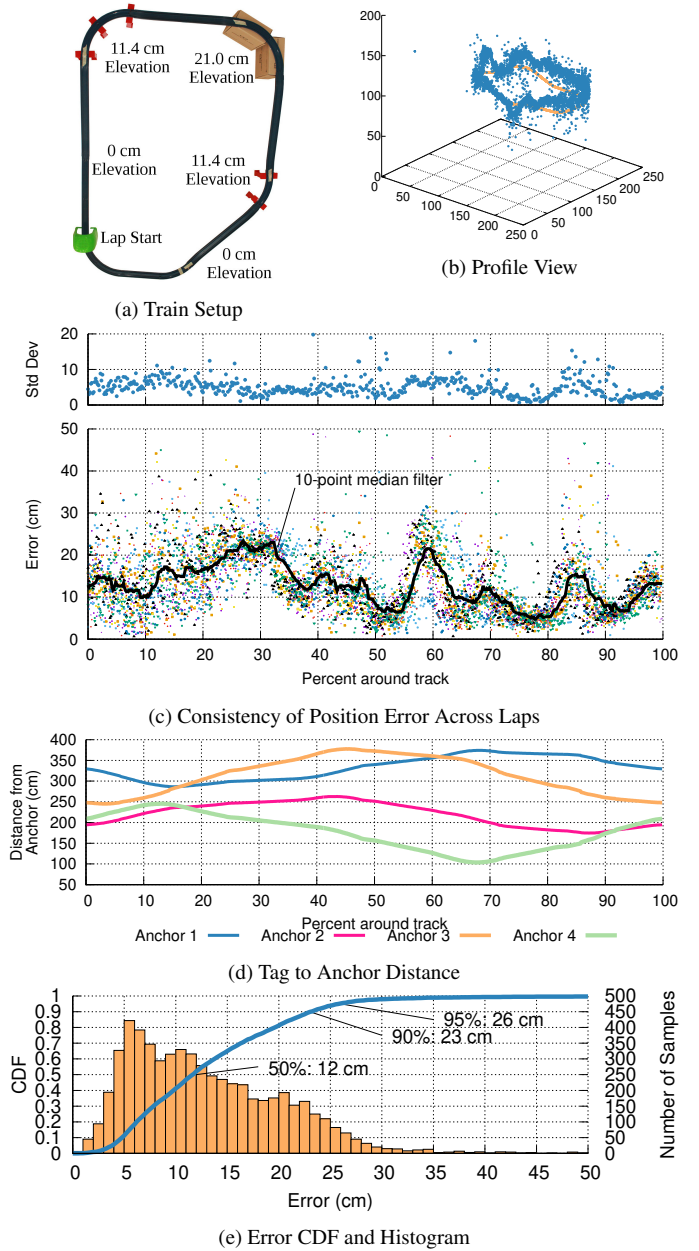### C. Consistency on a Static Path (Figure 10)

While the quadrotor experiment demonstrates Harmonium's ability to reconstruct a challenging arbitrary path, we are also interested in the reproducibility of Harmonium's position estimates over time. In Figure 10, we place a tag on a model train and record ten laps around the fixed track. During this experiment, we move about the space normally, perturbing the multipath environment between samples at the same point in space. Figure 10c shows an aggregate point cloud of all ten laps and the variation across laps. While the position error varies around the track, the variance is consistent at each location, that is the standard deviation of position error is relatively constant. This suggests that the measurement error has a physical root cause based on the properties of specific points in the space.

D. Pulse Generation and Regulatory Compliance (Figure 11)

As pulse generation quality leads directly to spectral usage, which in turn informs location quality, Figure 11 evaluates the expected and actual performance of Harmonium's pulse generation circuitry. The addition of the high-pass filter, necessary for regulatory compliance, abbreviates the tag's effective bandwidth. However, the design is still able to achieve nearly 3.5 GHz of bandwidth.

E. System Microbenchmarks

The Harmonium design expressly introduces an asymmetry between tags and anchors to minimize the burden of introducing Harmonium tags to devices to be localized. Here we quantify how burdensome the realized tag design is and the impact on the Harmonium anchor. The Harmonium tag is made of a 3.9×1.5 cm PCB with a 2.4×2.2 cm UWB antenna. The whole tag fits within a $3.9 \times 2.2 \times 0.2$ cm bounding box, or about 1.5 cm^3. The tag weighs only 3 g and draws only 75 mW. At a 19 Hz update rate, the tag uses 3.9 mJ per location estimate. The Harmonium anchors consist of a central 6.7×5.8 cm PCB with three 2.4×2.2 cm UWB antennas mounted co-planar at 120° offsets. One USRP1 can service up to two Harmonium anchors. The data from one USRP1 (two anchors) nearly saturates a USB 2.0 bus, requiring USB 3.0, more than two bus controllers, or multiple machines to support more than four Harmonium

(a) Train Setup

(b) Profile View

(c) Consistency of Position Error Across Laps

(d) Tag to Anchor Distance

(e) Error CDF and Histogram

Fig. 10: Point-cloud of location estimates and CDF of errors tracking ten laps of a model train around a track. Errors are consistent in space, implying a physical root cause.

anchors. One 3.2 GHz Xeon core can solve a position estimate in 231 ms. At least five parallel cores are required to keep up with Harmonium's 19 Hz update rate.

VI. DISCUSSION

This paper presents new tag and anchor designs which will help to improve the cost, complexity, and accuracy of current RF localization systems. Additionally, the choice of anchor ADC sampling rate, sweep rate, and overall sampling bandwidth allows for a customizable tradeoff between position estimation rate, accuracy, and system cost.

(a) Simulated Pulse

(b) Measured Pulse – No High Pass Filter

(c) Measured Pulse – With High Pass Filter

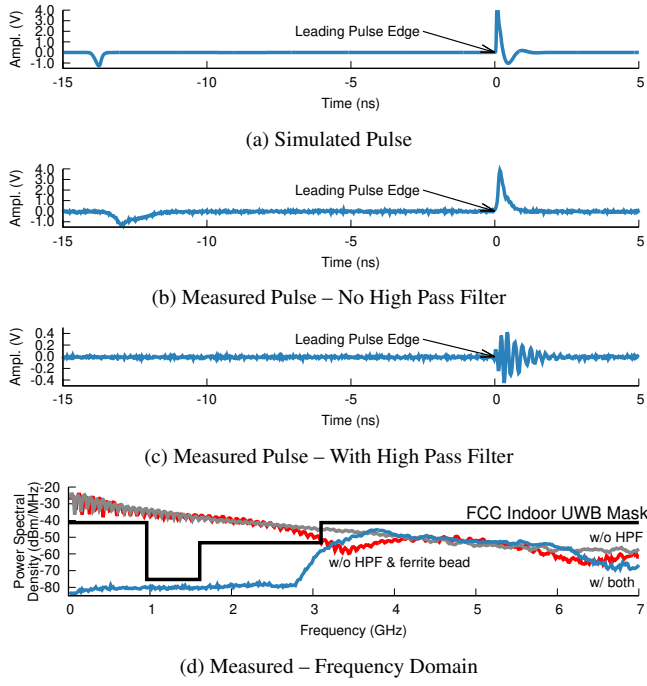

(d) Measured – Frequency Domain

Fig. 11: Simulated and measured time- and frequency-domain characteristics of the prototype pulse generator. The generated pulse is 275 ps wide (FWHM) and occupies more than 7 GHz of bandwidth. The frequency content below 3.1 GHz is stronger than allowed by FCC UWB guidelines, requiring the use of a high-pass filter to attenuate low-frequency content.

A. Limitations

Physical Limits. This paper has described a system tailored to tracking micro quadrotors and other small mobile objects in heavy multipath indoor environments. The resulting choice of a 4 MHz PRF limits the maximum channel delay spread to 250 ns. The power spectral limit of -41.3 dBm/MHz along with the LO frequency transition time between snapshots impose limitations on the maximum attainable position update rate.

Antenna Nulls and Cross-Polarization. The beam pattern for the antennas used in our evaluation includes nulls at the antenna's top and bottom [50]. Significant attenuation of the LOS path can occur when the incident path between tag and anchor falls into a null or the polarizations do not match. It is then difficult to distinguish the signal's time-of-arrival from the effects of much stronger multipath. To help mitigate this, Harmonium anchors employ antenna diversity (three antennas), yet significant attenuation can result if a whole anchor falls into one of the tag antenna's nulls. We speculate that this is the source for much of Harmonium's error.

Centralized Architecture. The current implementation expects a centralized controller with low-latency access to each anchor. This allows for tight timing synchronization between anchors and eases the hardware requirements for the purposes of this evaluation, but large-scale deployments would require a decentralized design.

Tight timing synchronization between anchors in a TDoA localization system is required due to the high propagation speed of RF signals through air. There exists no direct correlation between position error and synchronization error in a TDoA localization system as it depends on tag and anchor placement, but should at least exceed the ToA estimation accuracy exhibited by the system. As an example, 100 ps of simulated average clock synchronization error introduces 2 cm of average location bias for the unobstructed stationary data analyzed previously. Potential methods for accurate decentralized time synchronization have been explored in previous work using both wireless [56], [57] and wired techniques [58], [59].

The issue of decentralization could be ignored altogether if localization operations could be performed with only one anchor. Recent work has shown that multipath can be leveraged to perform localization with only one anchor if the position of reflective surfaces in the environment are known [60]. These same techniques could be leveraged by Harmonium, and has the potential to significantly reduce the deployment complexity if only one anchor is required for each indoor space.

B. Future Directions

Alternative Trigger Sources. Currently, a crystal oscillator triggers the tag's UWB pulses. However, the trigger only needs to be a CMOS-compatible signal. This opens up the possibility of utilizing PN codes to provide code-division multiple access (CDMA) schemes to allow for the simultaneous tracking of multiple targets. With multiple tags, a determination of PRF using frequency-domain methods such as those used by Harmonium is not possible. However, traditional CDMA time-domain receive techniques [66] could be used to determine the PN code delay across separate points in time, providing an accurate estimate of PRF.

Other CMOS sources might provide low datarate transmission. This could enable hybrid applications where localization is the key system component yet small amounts of tag to infrastructure data communication is still required.

Increasing Update Rate. Harmonium currently acquires ToA estimates from each anchor at 56 Hz. However, to minimize position error, anchors sequentially sample ToA across all three antennas. Therefore, the resulting position estimates are only obtained at $56/3 \approx 19$ Hz. Further analysis of the datasets presented in this paper shows that the best choice of antenna at each anchor has a high temporal correlation. An updated implementation may be able to increase the aggregate sampling rate to close to 56 Hz by only occasionally switching between antennas to determine if the best anchor has changed.

Anchor Placement. A cursory glance at Figure 9 and Figure 10 suggests that the majority of the error in position can be attributed to an inaccuracy in Z. Similar to the inaccuracy commonly found in GPS altitude estimation, this phenomenon is likely attributed to a vertical dilution of precision [67]. Like GPS, our anchor placements are biased towards the ceiling of the room and did not provide optimal coverage for the intended tracking area. Finding a means to unobtrusively deploy a floor-level anchor should help reduce error in Z.

Decreasing Tag Power. Up to 90 mA of instantaneous drive current is required to bring the tag's RF NPN transistor into saturation. The 68 pF capacitor seen in the tag's schematic in

System	Technology	LOS Precision	LOS Accuracy	Through-Wall Precision	Through-Wall Accuracy	Update Rate	Latency	Top Tag Speed	Tag Power	Tag Volume	Max Tag/ Anchor Dist
WASP [8]	NB (5.8 GHz) ToA	16.3 cm	50 cm (82%ile)	*Not Published*	50 cm (65%ile)	10 Hz	< 25 ms	Several m/s	2-2.5 W	*Not Published*	*Not Published*
LANDMARC [61]	Active RFID RSS	50% w/in 100 cm	< 200 cm	*Not Published*	*Not Published*	0.13 Hz	*Not Published*	< 1 m/s	N/A	~5 cm³	< 10 m
UbiSense [10]	UWB TDoA+AoA	99% w/in 30 cm	15 cm	*Not Published*	*Not Published*	33.75 Hz	*Not Published*	*Not Published*	*Not Published*	24.5 cm³	160 m
TimeDomain [9]	UWB TW-ToF	2.3 cm	2.1 cm	*Not Published*	"< 50 cm"	150 Hz	*Not Published*	*Not Published*	4.2 W	97 cm³	"hundreds of m"
FILA [4]	802.11 RSSI+CSI†	*Not Published*	45 cm (med)	*Not Published*	120 cm (med)	62.5 Hz	10 ms	> 1 m/s‡	1.6 W§	2.7 cm³¶	*Not Published*
Lazik et. al [12]	Ultrasonic TDoA	*Not Published*	3 cm (med) 12 cm (90%)	*Not Published*	*Not Published*	0.9 Hz	*Not Published*	*Not Published*	1.1 W¶¶	88 cm³	100 m
Harmonia [62]	UWB TDoA	*Not Published*	39 cm (med) 82 cm (90%)	*Not Published*	*Not Published*	56 Hz	*post-processed*	*Not Published*	120 mW**	*Not Published*	*Not Published*
Tagoram [19]	NB (UHF) SAR	*Not Published*	12.3 cm (med)	*Not Published* (Only known track)		At most 30 Hz	2500 ms	0.5 m/s	N/A	8 cm³	10 m
WiTrack [21]	UWB ToF	*Not Published*	12 cm (med) 31 cm (90%)	*Not Published*	15 cm (med) 40 cm (90%)	At most 400 Hz	75 ms	*Not Published*	N/A	32,700 cm³ (avg torso [63])	*(Not Published)* > 11 m
RF-IDraw [20]	NB (UHF) Interferometry	3.6 cm (med) 3.7 cm (90%)	19 cm (med) 38 cm (90%)	4.9 cm (med) 13.6 cm (90%)	32 cm (med) 48 cm (90%)	At most 53 Hz	< 500 ms§§	0.5 m/s*	N/A	8 cm³	9 m
PolyPoint [51]	UWB ToF	31 cm	39 cm (med) 140 cm (90%)	*Not Published*	*Not Published*	16 Hz	7 ms	*Not Published*	150 mW	9 cm³	50 m
Harmonium	**UWB TDoA**	**9 cm (med)** **16 cm (90%)**	**14 cm (med)** **31 cm (90%)**	**13 cm (med)** **38 cm (90%)**	**16 cm (med)** **42 cm (90%)**	**19 Hz**	**231 ms**	**2.4 m/s††**	**75 mW**	**1.5 cm³**	**78 m**

† CSI is Channel State Information, PHY layer metrics on each 802.11 subcarrier.   ‡ No upper bound given. Experiments run up to 1 m/s.

§ Using reported power numbers from [64] for Intel WiFi Link 5300 in RX mode.   ¶ Assuming smaller, PCIe Half Mini Card form factor.

¶¶ Estimate from power draw of similar audio+network apps [65]   †† Estimated as (56 Hz / 3.5 GHz×c) / 2

§§ The paper reports only "real-time", however this is as perceived by a human user, which may not be sufficient for applications such as controls.

* This paper reports no speed information, but uses the same tag and similar anchors as Tagoram, so we use the same top speed estimate.

** Published power draw of 8.5 mW is in addition to a traditional narrowband radio. This estimate adds a CC2520 as a representative low-power radio.

TABLE I: Comparison of localization quality, utility, and SWaP performance for recent high-performing indoor RF localization systems. Where possible, reasonable extrapolations are made. Harmonium achieves comparable localization performance with best in class systems, exceeding several in through-wall cases, with near-best SWaP metrics, from independent measurements capable of tracking faster-moving objects than nearly any other system.

Figure 6 selects the monopulse generator's pulse time. A careful evaluation to determine the minimum possible pulse duration would likely aid in significantly reducing tag power.

VII. RELATED WORK

As there is a very diverse breadth of localization technologies, we focus our comparison on ideological neighbors, other RF-based and UWB systems. Table I provides a summary comparison with recent state-of-the-art commercial and research localization systems. Additionally, as Harmonium is more than simply a localization system, we also survey related work in UWB pulse generation and signal recovery.

A. Narrowband Location Systems

Received signal strength indicator (RSSI) measurements can be used to determine the anchor-tag distance through direct analysis of received signal power. These systems rely on the power-law relationship between RSSI and tag-anchor distance. RSSI localization systems have the advantage of requiring little to no hardware modifications. However, their accuracy is limited due to the deep fades which are present in even the simplest multipath environments [2].

Due to the prevalence of narrowband radio technologies, e.g. WiFi, there have been countless attempts to develop systems which utilize just the bands available to traditional narrowband radios. In 2004, Elnahrawy et al. showed a fundamental limit on the order of meters for simple fingerprinting of the 2.4 GHz ISM band [68]. For many years, despite novel techniques and a wide range of efforts in this area, most narrowband systems have seen accuracies of at best half a meter due to their low-resolution view of the multipath environment [69], [70].

Recently, beamforming [71], synthetic aperture radar [5], [19], and interferometric [20] techniques have shown that narrowband localization technologies can best 0.5 m accuracy indoors.

These techniques, however, rely on non-static environments and measure *changes* in target position but either blindly preserve a static initial offset or retroactively learn true position after several seconds of motion. Furthermore, these systems rely on point-to-point state to feed models that predict viable motion paths to reject outliers and smooth estimates. Such application-specific optimizations are complementary and could also be applied to raw Harmonium estimates to further improve accuracy, but also require that any direct comparisons respect the difference between what is presented.

B. UWB Systems and Technology

UWB radio technologies have seen a great rise in interest since the FCC approved unlicensed usage in the 3.1 to 10.6 GHz band in 2002. Many methods have been proposed for the generation and detection of UWB signals. However, there has been little commercial realization of these technologies, severely limiting the possibility of the creation and evaluation of localization systems using UWB. Furthermore, UWB radios along with the state-of-the-art in research are predominantly chip-based designs, limiting the simple tweaking and modification necessary for design improvement and research.

1) Commercial UWB Technologies: Commercial UWB localization systems have thus far focused on tracking tools and inventory in industrial assembly centers. Tag power consumption runs on the order of watts, and with duty cycling and a modestly large battery the tags achieve lifetimes of one to a few months. The tags generally cost between $50-100 USD, while fitting a room with anchors quickly runs into thousands of dollars. These costs make widespread adaptation in broader environments difficult, and are largely driven by the high system complexity and costs associated with the direct sampling methods used for tag localization [9], [10].

Recently, DecaWave released an 802.15.4a (UWB) compliant radio that also supports time-based localization technologies [54]. Three systems built on DecaWave competed at the 2015 Microsoft Indoor Localization Competition, giving a baseline for performance. We compare with the overall 3rd place PolyPoint [51] as much more data is available from the follow-on publications and find that Harmonium is able to achieve $2\times$ better accuracy (14 cm median over 39 cm) and a comparable update rate (19 Hz vs 16 Hz) at half the power (75 mW vs 150 mW) and one sixth the size (1.5 cm^3 vs 9 cm^3).

2) UWB Transmitters and Pulse Generation: The generation of an accurate, stable stream of short pulses is critical to the operation of Harmonium. Fortunately, UWB pulse generation is a well-studied area, with multiple design options built around the step recovery effect. Other pulse generation techniques have also been studied which make use of high-speed comparators to create fast transition times, however these circuits have the disadvantage of high active power and moderately low bandwidth. Circuits based on the step recovery effect generally use step recovery diodes (SRDs) [72], BJTs [73], or SRDs with differentiators [37]. Designs that make use of SRDs come with the disadvantage that SRDs are hard to source. SRD pricing is typically around $30 to $40 per unit due to limited production quantity. BJT-based step recovery designs offer a clear advantage over SRDs due to their sub-$1 price point.

This paper builds upon previous step recovery designs by eliminating the need for the physically-large and unintuitive differentiator circuitry in prior work [36]. As Harmonium relies on the spectral content and not the short time-based properties, both the differentiator circuitry and Schottky diode are unnecessary and removed in favor of decreased tag complexity.

3) UWB Receivers and Pulse Detection: Prior to Harmonium, UWB pulse timing was traditionally performed in the time domain. Direct conversion receivers use high-speed ADCs to sample the UWB channel at or above the time resolution necessary for accurate time-of-arrival estimation. Although this allows for the highest performance in terms of position update rate, the ADCs and associated processing circuitry can be prohibitively costly. Energy detection receivers determine time-of-arrival by measuring the received pulse energy across short time intervals by successively sweeping the output of an energy detector across a bank of capacitors [74]. The resulting amount of charge contained in each capacitor is analyzed to determine the one that most likely contains the pulse's leading edge. While conceptually simple, energy detection receivers require custom circuit design and exhibit poor overall SNR performance. Sampling receivers also take small snapshots of time, but space the samples out over a period just longer than that of the pulse repetition frequency [36], [75]. This allows for an accurate reconstruction of the entire channel impulse response. However, sampling receivers are unable to directly filter out narrowband interference which may lead to reduced performance in complex RF environments.

VIII. CONCLUSIONS

This paper demonstrates that it is possible to localize small, fast-moving, airborne objects, like micro quadrotors, in heavily cluttered indoor environments without resorting to expensive and fragile optical motion capture systems and that such a system even works through the walls. To do so, we introduce Harmonium, an asymmetric localization system that employs inexpensive UWB tags and slightly-modified narrowband anchors which introduce a frequency-stepped bandstitching architecture to the UWB localization problem. Harmonium provides nearly unprecedented performance at a minimalist size, weight, and power point.

Having demonstrated the viability and accuracy possible with this approach, future work could establish the theoretical limits of the approach, support multiple concurrent devices, apply the basic design to imaging indoor environments, or explore efforts to improve update rate through parallelization. But, even without these explorations and enhancements, our design makes an inexpensive localization system accessible for a range of demanding applications today.

REFERENCES

[1] Y. Gu *et al.*, "A survey of indoor positioning systems for wireless personal networks," *Communications Surveys & Tutorials, IEEE*, vol 11, 1, 2009.
[2] Z. Farid *et al.*, "Recent advances in wireless indoor localization techniques and system," *Journal of Computer Networks and Communications*, 2013.
[3] P. Bolliger, "Redpin – adaptive, zero-configuration indoor localization through user collaboration," *Proceedings of the First ACM International Workshop on Mobile Entity Localization and Tracking in GPS-less Environments*, MELT'08, 2008.
[4] K. Wu *et al.*, "FILA: Fine-grained indoor localization," *INFOCOM, 2012 Proceedings IEEE*, 2012.
[5] S. Kumar *et al.*, "Accurate indoor localization with zero start-up cost," *Proceedings of the 20th Annual International Conference on Mobile Computing and Networking*, MobiCom'14, 2014.
[6] G. Conte *et al.*, "BlueSentinel: A first approach using iBeacon for an energy efficient occupancy detection system," *Proceedings of the 1st ACM Conference on Embedded Systems for Energy-Efficient Buildings*, BuildSys'14, 2014.
[7] E. Dhalgren *et al.*, "Evaluation of indoor positioning based on Bluetooth Smart technology," Master's thesis, Chalmers, Jun 2014.
[8] T. Sathyan *et al.*, "WASP: A system and algorithms for accurate radio localization using low-cost hardware," *IEEE Transactions on Systems, Man, and Cybernetics – Part C*, vol 41, 2, Mar. 2011.
[9] "Time Domain PulsON 400 RCM," Online.
[10] Ubisense, "Series 7000 Compact Tag," Online.
[11] S. P. Tarzia *et al.*, "Indoor localization without infrastructure using the acoustic background spectrum," *Proceedings of the 9th International Conference on Mobile Systems, Applications, and Services*, MobiSys'11.
[12] P. Lazik *et al.*, "Indoor pseudo-ranging of mobile devices using ultrasonic chirps," *Proceedings of the 10th ACM Conference on Embedded Network Sensor Systems*, SenSys'12, 2012.

[13] K. Klipp *et al.*, "Low cost high precision indoor localization system fusing intertial and magnetic field sensor data with radio beacons," Second Annual Microsoft Indoor Localization Competition, April 2015.

[14] C. Sánchez *et al.*, "STeAM sensor tracking and mapping," Second Annual Microsoft Indoor Localization Competition, April 2015.

[15] N. Rajagopal *et al.*, "Visual light landmarks for mobile devices," *Proceedings of the 13th International Symposium on Information Processing in Sensor Networks*, IPSN'14, 2014.

[16] Y.-S. Kuo *et al.*, "Luxapose: Indoor positioning with mobile phones and visible light," *The 20th Annual International Conference on Mobile Computing and Networking*, MobiCom'14, September 2014.

[17] S. Patel *et al.*, "PowerLine Positioning: A practical sub-room-level indoor location system for domestic use," UbiComp'06.

[18] Y. Mulgaonkar *et al.*, "Power and weight considerations in small, agile quadrotors," *SPIE Defense+Security*, 2014.

[19] L. Yang *et al.*, "Tagoram: Real-time tracking of mobile RFID tags to high precision using COTS devices," MobiCom'14, 2014.

[20] J. Wang *et al.*, "RF-IDraw: Virtual touch screen in the air using RF signals," SIGCOMM'14, 2014.

[21] F. Adib *et al.*, "3D tracking via body radio reflections," NSDI'14, 2014.

[22] D. Humphrey *et al.*, "Super-resolution time of arrival for indoor localization," *IEEE International Conference on Communications*, 2008.

[23] M. Verhelst *et al.*, "A reconfigurable, 0.13 μm CMOS 110 pJ/pulse, fully integrated IR-UWB receiver for communication and sub-cm ranging," *Solid-State Circuits Conference*, 2009.

[24] D. Lachartre *et al.*, "A 1.1 nJ/b 802.15.4a-compliant fully integrated UWB transceiver in 0.13 μm CMOS," *Solid-State Circuits Conference*, 2009.

[25] Y. Zheng *et al.*, "A 0.18 μm CMOS 802.15.4a UWB transceiver for communication and localization," *Solid-State Circuits Conference*, 2008.

[26] R. J. Duckworth *et al.*, "Radio design and performance analysis of multi carrier-ultrawideband (MC-UWB) positioning system," *Proc. Institute of Navigation, National Technical Meeting*, 2005.

[27] M. Segura *et al.*, "Experimental demonstration of self-localized ultra wideband indoor mobile robot navigation system," *International conference on indoor positioning and indoor navigation (IPIN)*, 2010.

[28] A. Feldman *et al.*, "Toward the deployment of an ultra-wideband localization test bed," *Vehicular Technology Conference*, 2011.

[29] M. B. Blanton, "An FPGA software-defined ultra wideband transceiver," Master's thesis, Virginia Tech, 2006.

[30] R. Blazquez *et al.*, "Digital architecture for an ultra-wideband radio receiver," *Vehicular Technology Conference*, vol 2, 2003.

[31] I. Lu *et al.*, "ADC precision requirement for digital ultra-wideband receivers with sublinear front-ends: A power and performance perspective," *VLSI Design*, 2006.

[32] S. Iida *et al.*, "A 3.1 to 5 GHz CMOS DSSS UWB transceiver for WPANs," *Solid-State Circuits Conference*, 2005.

[33] A. Azakkour *et al.*, "A new integrated monocycle generator and transmitter for ultra-wideband (UWB) communications," *Radio Frequency integrated Circuits (RFIC) Symposium*, 2005.

[34] H. Kim *et al.*, "All-digital low-power CMOS pulse generator for UWB system," *Electronics Letters*, vol 40, 24, 2004.

[35] H. Kim *et al.*, "A tunable CMOS UWB pulse generator," *Ultra-Wideband, The 2006 IEEE 2006 International Conference on*, 2006.

[36] S. Hantscher *et al.*, "Hardware concepts for the sequential sampling of repetitive pulse radar echoes in cost-efficient ultra-wideband transceivers," *Microwave and Optical Technology Letters*, vol 52, 3, 2010.

[37] J. Han *et al.*, "A new ultra-wideband, ultra-short monocycle pulse generator with reduced ringing," *Microwave and Wireless Components Letters, IEEE*, vol 12, 6, June 2002.

[38] H. Zhang *et al.*, "A novel UWB pulse generator," *Communications, Computers and Signal Processing (PacRim), 2011 IEEE Pacific Rim Conference on*. IEEE, 2011.

[39] Y. Guo *et al.*, "Novel design and implementation of ultra-wideband pulse generator based on avalanche transistor," *Session 1P0*, 2014.

[40] C. Zhang *et al.*, "Real-time noncoherent UWB positioning radar with millimeter range accuracy: Theory and experiment," *Microwave Theory and Techniques, IEEE Transactions on*, vol 58, 1, 2010.

[41] W. Namgoong, "A channelized digital ultrawideband receiver," *Wireless Communications, IEEE Transactions on*, vol 2, 3, 2003.

[42] S. Hoyos *et al.*, "Ultra-wideband analog-to-digital conversion via signal expansion," *Vehicular Technology, IEEE Transactions on*, vol 54, 2005.

[43] J. Xiong *et al.*, "ToneTrack: Leveraging frequency-agile radios for time-based indoor wireless localization," *Proceedings of the 21st Annual Int. Conference on Mobile Computing and Networking*. ACM, 2015.

[44] E. J. Candès *et al.*, "Robust uncertainty principles: Exact signal reconstruction from highly incomplete frequency information," *Information Theory, IEEE Transactions on*, vol 52, 2, 2006.

[45] R. Bucher *et al.*, "A synthesizable VHDL model of the exact solution for 3D hyperbolic positioning system," *VLSI Design*, vol 15, 2002.

[46] Y. Chan *et al.*, "A simple and efficient estimator for hyperbolic location," *Signal Processing, IEEE Transactions on*, vol 42, 8, 1994.

[47] D. Z. Thai *et al.*, "Speaker localisation using time difference of arrival," DTIC Document, Tech. Rep., 2008.

[48] M. S. Brandstein *et al.*, "A closed-form location estimator for use with room environment microphone arrays," *Speech and Audio Processing, IEEE Transactions on*, vol 5, 1, 1997.

[49] M. Gerding *et al.*, "Generation of short electrical pulses based on bipolar transistors," *Advances in Radio Science*, vol 2, 1, 2005.

[50] R. Azim *et al.*, "Compact tapered-shape slot antenna for UWB applications," *Antennas and Wireless Propagation Letters, IEEE*, vol 10, 2011.

[51] B. Kempke *et al.*, "PolyPoint: Guiding indoor quadrotors with ultra-wideband localization," *2015 ACM Workshop on Hot Topics in Wireless*, HotWireless '15, September 2015.

[52] "USRP1 Bus Series, Ettus Research LLC," Online.

[53] NaturalPoint, "OptiTrack." Available: Online

[54] DecaWave, "ScenSor DW1000," Online.

[55] Bitcraze, "The Crazyflie Nano Quadcopter." Available: Online

[56] R. Exel, "Clock synchronization in IEEE 802.11 wireless LANs using physical layer timestamps," *Precision Clock Synchronization for Measurement Control and Communication (ISPCS)*, 2012.

[57] C. McElroy *et al.*, "Comparison of wireless clock synchronization algorithms for indoor location systems," *Communications Workshops (ICC), IEEE*, 2014.

[58] P. Loschmidt *et al.*, "Highly accurate timestamping for ethernet-based clock synchronization," *Journal of Computer Networks and Comm.*, 2012.

[59] R. Exel *et al.*, "Asymmetry mitigation in IEEE 802.3 ethernet for high-accuracy clock synchronization," *Instrumentation and Measurement, IEEE Transactions on*, vol 63, 3, 2014.

[60] P. Meissner *et al.*, "Multipath-assisted single-anchor indoor localization in an office environment," *Systems, Signals and Image Processing (IWSSIP), 2012 19th International Conference on*. IEEE, 2012.

[61] L. Ni *et al.*, "LANDMARC: Indoor location sensing using active RFID," *Wireless Networks*, vol 10, 6, 2004.

[62] B. Kempke *et al.*, "Harmonia: Wideband spreading for accurate indoor RF localization," *2014 ACM Workshop on Hot Topics in Wireless*, HotWireless '14, September 2014, workshops.

[63] C. E. Clauser *et al.*, "Weight, volume, and center of mass of segments of the human body," Air Force Systems Command, Tech. Rep., 1969.

[64] D. Halperin *et al.*, "Demystifying 802.11n power consumption," *Proceedings of the 2010 International Conference on Power Aware Computing and Systems*, HotPower'10, 2010.

[65] Y. M. Kwete, "Power consumption testing for iOS," Master's thesis, North Dakota, October 2013.

[66] D. Divsalar *et al.*, "Improved parallel interference cancellation for CDMA," *Communications, IEEE Transactions on*, vol 46, 2, 1998.

[67] R. B. Langley, "Dilution of precision," *GPS world*, vol 10, 5, 1999.

[68] E. Elnahrawy *et al.*, "The limits of localization using signal strength: A comparative study," *Sensor and Ad Hoc Comm. and Networks*, Oct 2004.

[69] S. Lanzisera *et al.*, "Radio frequency time-of-flight distance measurement for low-cost wireless sensor localization," *Sensors Journal, IEEE*, 2011.

[70] P. Bahl *et al.*, "RADAR: An in-building RF-based user location and tracking system," vol 2, Mar. 2000.

[71] J. Xiong *et al.*, "ArrayTrack: A fine-grained indoor location system," *Usenix NSDI*, 2013.

[72] J.-S. Lee *et al.*, "Novel low-cost ultra-wideband, ultra-short-pulse transmitter with MESFET impulse-shaping circuitry for reduced distortion and improved pulse repetition rate," *Microwave and Wireless Components Letters, IEEE*, vol 11, 5, May 2001.

[73] D. Wentzloff *et al.*, "A 3.1-10.6 GHz ultra-wideband pulse-shaping mixer," *Radio Freq. Integrated Circuits (RFIC) Symposium*, June 2005.

[74] K. M. S. Thotahewa *et al.*, "Hardware architectures for IR-UWB-based transceivers," *Ultra Wideband Wireless Body Area Networks*, 2014.

[75] J. Han *et al.*, "On the development of a low-cost compact planar integrated-circuit sampling receiver for UWB sytems," *Ultra-Wideband Short-Pulse Electromagnetics 8*, 2007.